

Radio Pulsar Style Timing of Eclipsing Binary Stars from the ASAS Catalogue

S. K. Kozłowski^{1,2*}, M. Konacki^{1,2†} and P. Sybilski^{2‡}

¹*Adam Mickiewicz University, Astronomical Observatory, Poznań, Poland*

²*Nicolaus Copernicus Astronomical Center, Toruń, Poland*

Received...

ABSTRACT

The Light-Time Effect (LTE) is observed whenever the distance between the observer and any kind of periodic event changes in time. The usual cause of this distance change is the reflex motion about the system's barycenter due to the gravitational influence of one or more additional bodies. We analyze 5032 eclipsing contact (EC) and detached (ED) binaries from the All Sky Automated Survey (ASAS) catalogue to detect variations in the times of eclipses which possible can be due to the LTE effect. To this end we use an approach known from the radio pulsar timing where a template radio pulse of a pulsar is used as a reference to measure the times of arrivals of the collected pulses. In our analysis as a template for a photometric time series from ASAS, we use a best-fitting trigonometric series representing the light curve of a given EC or ED. Subsequently, an O–C diagram is built by comparing the template light curve with light curves obtained from subsets of a given time series. Most of the variations we detected in O–Cs correspond to a linear period change. Three show evidence of more than one complete LTE-orbit. For these objects we obtained preliminary orbital solutions. Our results demonstrate that the timing analysis employed in radio pulsar timing can be effectively used to study large data sets from photometric surveys.

Key words: binaries: eclipsing – methods: numerical.

1 INTRODUCTION

The fact that the velocity of light is finite was not obvious till 1676 when Olaus Roemer carried out precise measurements of the times of eclipses of Jovian moons. He noted that Io eclipses were "early" before opposition and "late" after opposition when compared to the *Ephemerides Bononiensis Mediceorum Siderum*, a work by Cassini published in 1668. It includes tables of times of eclipses of Jovian moons which were used to determine the differential longitude by simultaneous observations of the same eclipse from two places. Roemer's conclusion, though not a quantitative one, became a great discovery contradicting the Aristotelean thought. He provided scientists with the basics of the O–C (observed minus calculated) procedure (Sterken 2005b) and was the first one to analyze the effects caused by finite light speed, hereafter called the light time effect (LTE).

Below we analyze the photometric data from the All Sky Automated Survey, (ASAS; Pojmanski 2002). In §2 we present our method for analyzing the timing variations. In §3

we show the outcome of applying our approach to the photometric series of 5032 eclipsing contact (EC) and detached (ED) binaries from ASAS. In §4 we discuss several interesting cases of most likely the LTE effect due to companions to the analyzed systems and conclude in §5.

2 AUTOMATED TIMING OF ECLIPSING BINARIES

Our basic concept of detecting timing variations in photometry of ED/EC in an automated way is based on the method used in radio pulsar timing. It consists of six steps which are shown as a block diagram in Fig. 1.

(i) **Get a raw data set.** It is assumed that a raw data set consists of n magnitudes (or fluxes), their errors and the times they were recorded.

(ii) **Prepare a template light-curve model.** A raw data set is phased with the known period and the parameters of a template light-curve model are calculated using the least squares method. At this stage the period can be improved or corrected during the fitting process. This is often necessary for the ASAS data.

(iii) **Divide a raw data set into subsets.** A raw data

* E-mail: stan@ncac.torun.pl

† E-mail: maciej@ncac.torun.pl

‡ E-mail: sybilski@ncac.torun.pl

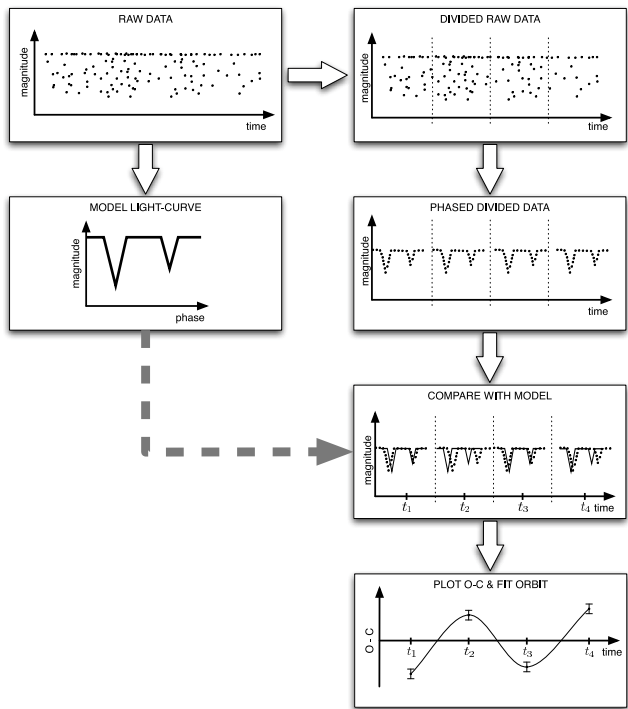


Figure 1. A block diagram describing our eclipse timing procedure.

set is divided into M intervals. The intervals can be equal in terms of the number of data points they include or the time that they span. The second variant was chosen in this paper. The intervals can be overlapping or have a non-repeating content. When implementing the first method, appropriate corrections must be applied when calculating the final formal errors due to a multiple usage of the same data points.

(iv) **Phase data in each interval.** Data points are phased separately in each interval using the new period value calculated during the creation of the model. The zeropoint is retained for each interval. This way a *local light-curve* is created and the mid-time of each interval is associated with it.

(v) **Compare with the template light-curve model.** The most important step in this procedure is the comparison of the *local light-curves* with the template light-curve model. At this stage a one-parameter least squares fit is performed in order to find the time shift between the two light curves.

(vi) **Plot an O–C diagram, fit an LTE orbit.** Finally, the collected O–C values can be plotted against time and, if possible, an orbit can be fitted.

2.1 A template light-curve model

We have tested two representations for a template model light curve — a polynomial model and a harmonic model. We have decided to use a harmonic model. Such an approach, apart from providing a good model of the input data, enables us to conveniently adjust the initial period of a binary. The model is based on a Fourier series and involves

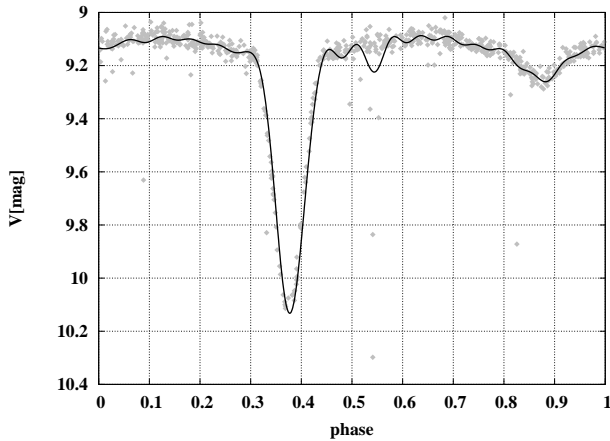


Figure 2. An example template light-curve model (solid line) calculated for ASAS 023539-4504.2 raw data. Note that the solid curve approximates the primary minimum very well despite oscillations visible between eclipses.

fitting a trigonometric series to a raw photometric data set:

$$f(t) = \frac{a_0}{2} + \sum_{l=1}^N \left[a_l \cos\left(\frac{2\pi}{T}lt\right) + b_l \sin\left(\frac{2\pi}{T}lt\right) \right]. \quad (1)$$

N has to be chosen so that the resulting light-curve model defined by the coefficients $a_0 \dots a_N$, $b_1 \dots b_N$ and the period T approximate the raw data as good as possible. Theoretically, the more harmonics are used (big N), the better the approximation. N has an upper limit though. Obviously, as a least squares algorithm is used to fit $f(t)$, the number of parameters cannot exceed the number of data points used in a fitted, i.e. $m = 2N + 2 < n$. Moreover, if m is close to n , the fit starts to approximate the data noise. This is not a desired effect. In our analysis we used $N = 18$ which was found to be the best for the types of curves analyzed. An example template model along with the original light-curve are presented in Fig. 2. Though it might seem that a lower value of N would make the model less sensitive to erroneous data points, at the same time the real eclipses (especially deep and short ones) would not have been modeled well enough. Having the primary eclipse well modeled is crucial when searching for time shifts between the model and the local light curves. If one would have high quality photometry it would then be good to optimize the procedure and select N individually for each object. In order to carry out the least-squares fitting we used the Levenberg-Marquardt algorithm and its Minpack¹ implementation.

2.2 Calculating O–C

Having the light curve model in form of T and $a_0 \dots a_N$, $b_1 \dots b_N$ coefficients, it can be compared with local light curves in each interval. This is done by fixing the parameters describing the model in Eqn. (1) and slightly modifying the

¹ <http://netlib.org/minpack/>

formula by introducing a time shift parameter t_O :

$$f_O(t) = \frac{a_0}{2} + \sum_{l=1}^N \left[a_l \cos\left(\frac{2\pi}{T}l(t - t_O)\right) + b_l \sin\left(\frac{2\pi}{T}l(t - t_O)\right) \right]. \quad (2)$$

Then, using least squares, $f_O(t)$ is fitted to local light curves with t_O as the only parameter. Effectively, t_O is the value of O–C at the given point in time. Collecting these for all intervals allows one to obtain a O–C diagram. Since Eqn. (2) is fitted using the Levenberg-Marquardt as before, the formal errors of the obtained O–C values are derived from the covariance matrix, which, in this case is a one-element matrix due to the fact that the fit has only one parameter.

2.3 Detection Criterion

Inspecting visually every single O–C diagram is not practical, hence in order to find binaries with significant timing variations we use the following timing activity parameter r

$$r = \frac{S}{A} > r_{min}, \quad (3)$$

where S is the standard deviation of the O–C values and A is the average error ($\Delta(O - C)$) of these values:

$$A = \frac{1}{M} \sum_{l=1}^M \Delta(O - C)_l. \quad (4)$$

Objects having r greater than a certain r_{min} are considered interesting. We applied the above criterion on data sets divided into 5-, 6-, 7- and 8-intervals. If an object passes the criterion at least once, it is considered interesting. Such objects are finally inspected visually.

3 TIMING VARIATIONS OF ED AND EC BINARIES FROM THE ASAS CATALOGUE

The *ASAS Catalogue of Variable Stars* (ACVS) is publicly available for download from the ASAS Project homepage². We used its version 1.1 in this paper. The catalogue consists of 50124 objects showing variability in brightness. Among them 2761 are uniquely classified as eclipsing contact (EC) binaries and 2271 as eclipsing detached (ED) binaries. Based on the original ACVS index file, we created two subindex files: one containing only EC binaries and a second one containing only ED binaries. This reduced the number of investigated light-curves to 5032. In the analysis only an A-rated³ photometry was taken into account. The results for ED are collected in Table 1. It lists 29 binaries. For this table we used $r_{min} = 2.0$. The results for EC are collected in Table 2. It contains 44 objects. In this case we used $r_{min} = 2.5$. The most frequent variation in O–C in both cases has a parabolic shape indicating a linear change in period. The r_{min} threshold has been adjusted individually for each type of curves (ED and EC). In case of contact binaries the eclipses are

² <http://www.astrouw.edu.pl/asas/>

³ The ACVS rates the quality of each brightness measurement on a scale from A to D with A being the best and D the worst quality.

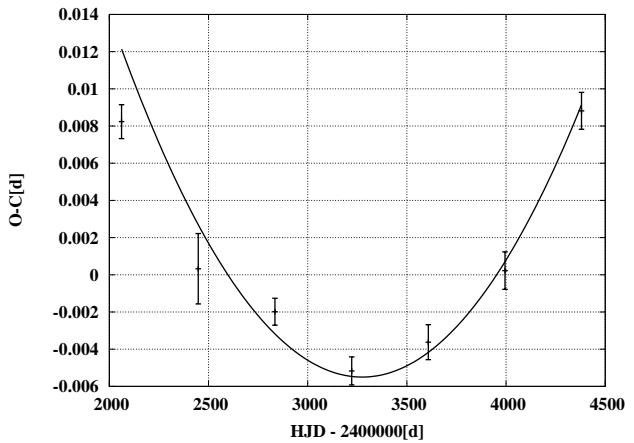


Figure 3. ASAS 060557-5342.9’s timing variations. The parabola corresponds to \dot{P} from Pilecki et al. (2007).

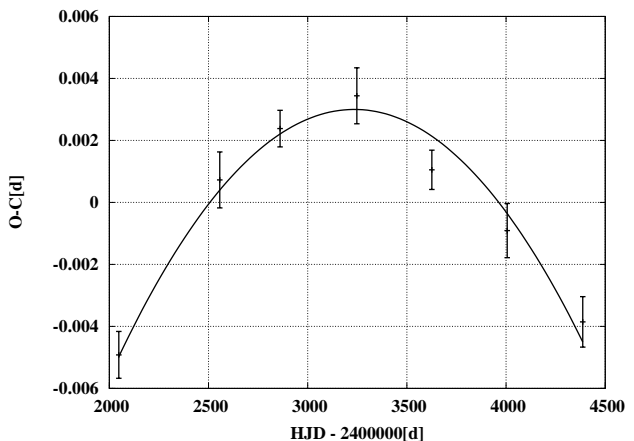


Figure 4. ASAS 160302-3749.4’s timing variations. The parabola corresponds to \dot{P} from Pilecki et al. (2007).

generally shallower and less sharp than in case of detached binaries - this results in different sensitivities of the algorithm in the two cases.

Recently Pilecki et al. (2007) have found EC binaries with high period change rates (HPCR) in the ASAS data. They have published a list of 31 stars exhibiting large \dot{P} . 10 out of 44 objects listed in Tab. 2 have been detected by Pilecki et al. (2007). Of the remaining 21 HPCR objects, 12 were classified as other than EC hence they were not analyzed by us. Finally, 9 objects did not satisfy our criterion. In order to verify that the results obtained with our proposed algorithm are consistent with Pilecki et al. (2007), we compared objects with high \dot{P} from the HPCR list with our timing measurements. This is demonstrated in Figures 3-4 by plotting the linear \dot{P} (i.e. parabolic in O–C) trend from Pilecki et al. (2007) together with our timing measurements. We have also extended the O–C diagram from Pilecki et al. (2007) for VY Cet, a contact binary system with the well known O–C variations. Qian (2003) studied this object and found the period of the third body to be 7.3 years with a minimum mass of $0.62M_{\odot}$. Figure 5 shows the original O–C diagram with our results overlotted.

ASAS ID	P [d] (ASAS)	P [d] (corrected)	r_5	r_6	r_7	r_8	Other ID
034746-0836.7	2.8764	2.8768183	3.58	1.66	2.11	2.15	CD Eri
050205-2842.8	3.3023	3.3024868	2.01	2.73	1.73	1.91	-
053727-7752.3	0.99158	0.9915804	3.14	2.74	2.25	1.92	-
070825-4433.2	1.8519	1.8518267	2.17	1.97	1.15	2.24	-
071021-3324.6	1.657725	1.6577068	2.07	2.18	1.15	0.89	CI Pup
090039-4739.8	4.4045	4.4047483	2.09	2.16	1.95	1.56	-
092456-3337.2	1.44643	1.4464050	2.42	2.23	2.45	1.15	SV Pyx
094542-4913.5	1.552517	1.5525371	3.00	3.38	3.27	1.86	DU Vel
111915-1949.7	2.3409	2.3410108	3.80	3.71	3.10	2.33	RV Crt
121103-5040.3	1.9508	1.9507456	2.28	2.05	1.87	1.58	NSV05487
121158-5050.7	1.135683	1.1356929	2.16	2.03	1.63	2.15	NSV05497
130155-5040.7	3.511604	3.5117345	2.96	2.03	1.88	1.94	NSV06061
130856-7437.6	1.479905	1.4799275	2.44	2.49	2.75	2.21	-
132107-1936.4	3.042031	3.0420286	2.71	2.45	1.48	1.32	-
132402-6345.9	1.737062	1.7370648	5.64	5.36	4.32	4.09	-
132538-2025.0	0.47849	0.4784917	2.30	1.99	1.90	1.86	-
141035-4546.8	0.988708	0.9887115	2.04	1.86	1.85	1.42	-
143636-5124.8	1.45313	1.4530916	1.84	1.71	2.01	1.68	DT Lup
154645-2307.5	1.281968	1.2819585	2.87	2.43	2.00	2.36	-
161628-0658.7	2.446109	2.4461205	3.03	2.04	1.99	1.59	SW Oph
171519-3639.0	2.41344	2.4134785	2.05	1.50	1.47	1.99	V0467 Sco
174303-3222.3	2.192577	2.1925951	2.93	1.63	1.65	1.33	V0496 Sco
191350+1109.8	0.334838	0.3348409	1.76	1.58	2.04	2.02	-
193840-4500.6	1.35187	1.3518939	2.73	2.97	2.96	1.69	V0795 Sgr
200048-2833.4	1.665189	1.6651979	3.87	2.57	2.47	1.22	V1173 Sgr
205101-6341.5	2.5442	2.5441900	2.68	1.23	1.01	1.16	BT Pav
213148-4502.7	1.880496	1.8805027	1.57	2.23	1.94	1.67	U Gru
215704-5606.0	0.454887	0.4548896	1.90	2.00	1.66	1.05	-
223621-1116.4	1.62854	1.6285257	2.70	1.36	1.71	2.02	-

Table 1. LTE search results: ASAS ED objects. The table lists the object’s ID, the period value from the ACVS catalogue, a corrected period obtained during reference model computation. Four r values for 5-, 6-, 7- and 8-interval runs are given. The last column contains other IDs, if any.

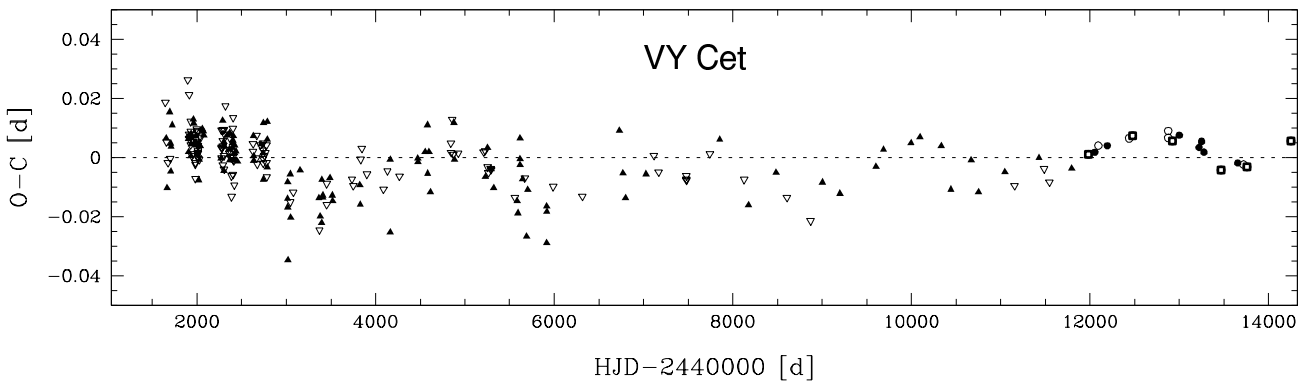


Figure 5. The timing variations of VY Cet. This O–C diagram is from Pilecki et al. (2007). Our timing variations are denoted with squares.

4 ECLIPSING BINARIES WITH LTE ORBITS — ASAS 123244-8726.4, ASAS 075809-4648.5 AND ASAS 141035-4546.8

During a visual inspection of the detected timing variations we identified three interesting cases most likely corresponding to an LTE effect due to a third companion. We subsequently analyzed them using a modified version of our approach. It differs from the original one described above in the way the intervals are chosen. Rather than setting the

number of intervals, this time, the length of the intervals (in days) and the shift between them (in days) are used as parameters. This enables one to create overlapping intervals. E.g. choosing a length of an interval of 300 days and setting the shift between intervals to 100 days produces 30 intervals assuming that the time span is 3200 days. An important difference is that data points are used multiple times for an O–C computation. This way it is possible to produce an infinite number of points in the O–C diagram having the same input data as in the standard algorithm. The statis-

ASAS ID	P [d] (ASAS)	P [d] (corrected)	r_5	r_6	r_7	r_8	Other ID
002449-2744.3	0.31367	0.3136602	3.10	2.71	2.35	2.66	-
004240-2956.7	0.301682	0.3016864	3.49	3.15	2.29	3.25	-
030313-2036.9	0.334978	0.3349778	2.69	2.63	1.38	2.19	TU Eri
030315-2311.2	0.4566	0.4566055	2.85	2.56	2.26	1.99	-
030617-6812.5	0.41612	0.4161200	4.35	4.23	3.77	3.97	NSV01054
032812-2503.5	0.315501	0.3155051	2.64	2.63	1.81	2.22	-
043046-4813.9	0.35714	0.3571467	3.59	3.56	2.19	3.06	-
050922-1932.5	0.270842	0.2708428	3.04	2.58	1.83	2.18	-
051114-0833.4	0.4234	0.4234030	4.47	3.79	3.30	3.21	ER Ori
052313-0907.7	0.40198	0.4019834	4.40	3.69	2.21	2.38	-
054000-6828.7	0.36222	0.3622215	2.79	2.76	2.31	3.03	ASAS 054000-6828.6
055501-7241.6	0.343841	0.3438400	3.21	2.96	2.96	3.02	BV 435
060557-5342.9	0.46363	0.4636373	4.61	4.45	3.48	3.03	-
061654-4326.4	0.504735	0.5047355	3.98	3.51	2.14	2.88	-
062254-7502.0	0.257704	0.2577062	5.18	5.28	5.24	4.91	-
064047-8815.4	0.43863	0.4386210	4.31	3.62	3.06	3.56	-
065232-2533.5	0.418634	0.4186402	2.79	2.63	1.98	2.13	-
070225-2845.8	0.462724	0.4627283	5.89	4.82	4.49	4.36	-
070232-5214.6	0.407338	0.4627283	5.89	4.82	4.49	4.36	-
070943-0702.3	0.501369	0.5013665	3.58	3.05	2.28	2.28	-
071727-4007.7	0.320267	0.3202645	4.46	4.55	3.09	3.62	GZ Pup
074308-1915.5	0.403302	0.4033032	3.78	3.84	2.91	3.22	-
075809-4648.5	0.390387	0.3903834	5.01	5.38	3.81	4.47	NSV03836
082030-4326.7	0.37078	0.3707788	3.02	3.00	2.33	2.22	-
082456-4833.6	0.364879	0.3648710	6.88	5.69	4.86	3.67	-
083139-4227.5	0.302677	0.3026776	3.00	2.75	3.28	2.34	NSV04126
084304-0342.9	0.348563	0.3485601	3.70	3.63	4.09	3.34	-
093312-8028.5	0.406071	0.4060657	6.59	5.22	3.11	4.97	-
095048-6723.3	0.276944	0.2769428	2.64	2.74	2.04	2.30	NSV04657
102552-3224.3	0.33706	0.3370613	2.80	2.65	2.63	2.46	-
114757-6034.0	1.65764	1.6575598	4.25	3.59	3.11	3.16	SV Cen
123244-8726.4	0.338519	0.3385238	4.58	8.81	7.25	6.93	NSV 5654
131032-0409.5	0.311251	0.3112486	3.14	3.04	2.49	2.57	-
143103-2417.7	0.287859	0.2878586	3.19	2.75	2.34	2.51	-
144226-4558.1	0.251557	0.2515636	3.29	2.75	2.20	2.69	-
145124-3740.7	1.301836	1.3017970	2.93	2.78	2.37	2.62	V0678 Cen
150452-3757.7	0.374131	0.3741329	3.28	3.03	2.90	3.33	NSV06917
153152-1541.1	0.358259	0.3582558	2.36	2.55	3.46	3.73	VZ Lib
184644-2736.4	0.302836	0.3028365	3.47	2.70	2.24	2.64	-
195004-5146.7	0.87546	0.8754432	3.57	3.55	3.44	3.90	V0343 Tel
195350-5003.5	0.286828	0.2868259	6.96	5.85	4.40	5.92	NSV12502
202438-5244.0	0.31593	0.3159329	3.14	2.77	2.32	2.19	NP Tel
213519-2722.8	0.3689	0.3689034	2.76	2.60	2.18	1.89	-
230749-2202.8	0.48431	0.4843096	6.19	6.33	4.78	4.52	-

Table 2. LTE search results: ASAS EC objects. The table lists the object’s ID, the period value from the ACVS catalogue, a corrected period obtained during reference model computation. Four r values for 5-, 6-, 7- and 8-interval runs are given. The last column contains other IDs, if any.

tical significance of these points is obviously appropriately lower than in the case of non-overlapping intervals and this must be taken into account when deriving formal errors. The main purpose of such an approach is to investigate how the O–C diagram looks between the points calculated using the standard algorithm and also how this influences the best-fitting LTE orbit.

ASAS 123244-8726.4, also known as NSV5654 is an EC binary that has a period of $0^d.338519$. It has been identified with high values of r reaching 8.81 in a 6-interval run. The O–C plot is shown in Fig. 6. A linear trend introduced by an imprecise period was removed by applying a period correction obtained from an orbital fit which included a correction to the period dP as one of the parameters. The O–C dia-

gram calculated using the new period shows evidence of an LTE orbit. Three complete cycles seem to be visible. The final orbital parameters are summarized in Tab. 3.

Another interesting EC object is ASAS 075809-4648.5 or NSV03836. This binary, having a period of $0^d.390383$, reveals periodic variability in the O–C diagram. As in the previous case, we used the standard (circles with error bars, solid line) and the overlapping method. Figure 7 shows two sets of O–C data points as well as two corresponding orbital solutions. Parameters are shown in Tab. 3.

ASAS 141035-4546.8 is the only object among analyzed ED systems that appears to exhibit periodic (O–C) variations with a period clearly shorter than the data time span. The eclipsing system has a period of $0^d.988708$. Figure 8

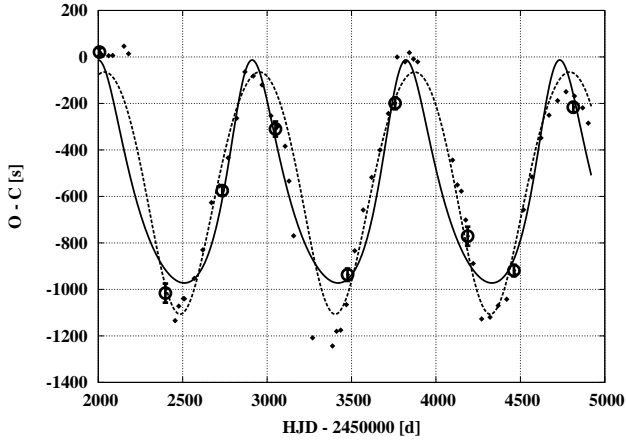


Figure 6. ASAS 123244-8726.4. The O-C diagram was obtained using the standard (circles with error bars, solid line) and the overlapping methods. Orbital solutions were fitted to both data sets.

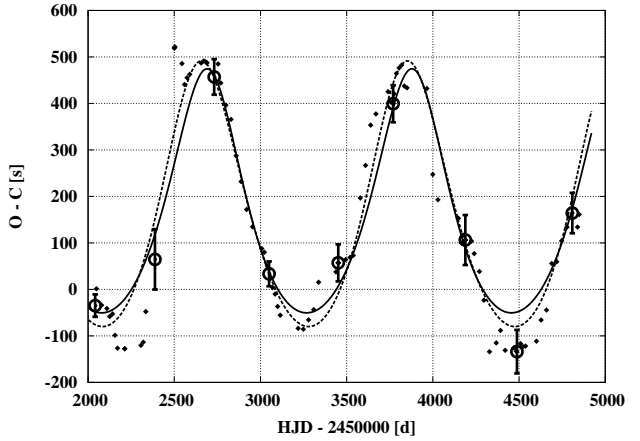


Figure 7. ASAS 075809-4648.5. The O-C diagram was obtained using the standard (circles with error bars, solid line) and the overlapping methods. Orbital solutions were fitted to both data sets.

parameter	unit	standard method	overlapping method
ASAS 123244-8726.4			
P	[d]	911 ± 5	918.4
$a \sin I$	[AU]	0.961 ± 0.024	1.042
e	–	0.159 ± 0.019	0.055
ω	[deg]	113 ± 8	0.98
T_0	[HJD]	2450143 ± 17	2450877
$f(m_{1,2}, m_3)$	$[M_\odot]$	0.143 ± 0.011	0.179
RMS	[s]	67.8	–
χ^2	–	3.65	–
k	–	3	–
ASAS 075809-4648.5			
P	[d]	1188 ± 27	1196
$a \sin I$	[AU]	0.52 ± 0.04	0.57
e	–	0.131 ± 0.052	0.098
ω	[deg]	84 ± 24	102
$f(m_{1,2}, m_3)$	$[M_\odot]$	0.0133 ± 0.0031	0.0173
T_0	[HJD]	2450328 ± 80	2450234
RMS	[s]	40.77	–
χ^2	–	1.43	–
k	–	3	–
ASAS 141035-4546.8			
P	[d]	1286 ± 120	1165
$a \sin I$	[AU]	0.76 ± 0.13	0.84
e	–	0.0	0.32
ω	[deg]	–	–
T_0	[HJD]	2450292 ± 122	2450154
$f(m_{1,2}, m_3)$	$[M_\odot]$	0.035 ± 0.019	0.043
RMS	[s]	156.15	–
χ^2	–	2.23	–
k	–	2	–

Table 3. LTE orbital parameters: period (P), projection of the semimajor axis a on the line of sight ($a \sin I$, I is the orbit's inclination), eccentricity (e), argument of periaapsis (ω), mass function ($f(m_{1,2}, m_3)$) for ASAS 123244-8726.4, 075809-4648.5 and 141035-4546.8 computed using data from the standard and the overlapping method. RMS, χ^2 and the degrees of freedom (k) have been calculated for the standard method.

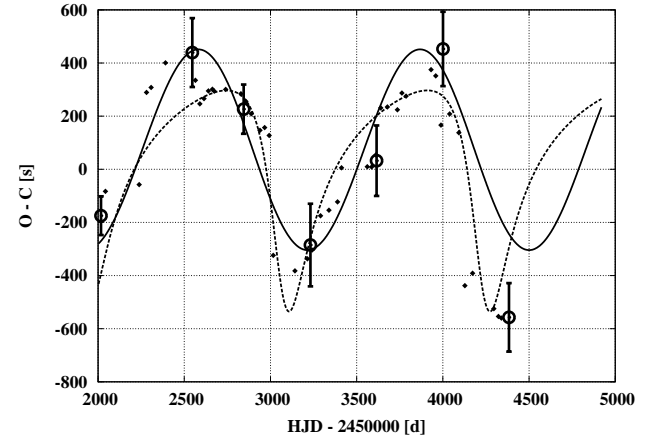


Figure 8. ASAS 141035-4546.8. The O-C diagram was obtained using the standard (circles with error bars, solid line) and the overlapping methods. Orbital solutions were fitted to both data sets.

shows two sets of the O-C points as well as two corresponding orbital solutions. In the case of the orbit fitted to the points obtained with the standard method, a circular orbit was assumed. Table 3 provides the orbital parameters.

The above analysis of three interesting cases shows the usefulness of the proposed methods. The standard algorithm is well suited for detection and general O-C computation while the second method based on overlapping intervals does the interpolation. It is not an interpolation in a strict mathematical sense though. There is no model (linear, cubic, spline, etc.) – O-C values are calculated accordingly to the actual trend in the data set. As shown in the examples, such interpolation can influence the shape of the fitted orbit. The eccentricity is the most sensitive parameter. $a \sin I$ and P do not differ much when comparing these two approaches.

5 CONCLUSIONS

Eclipsing detached and eclipsing contact binaries were investigated. Altogether 5032 objects have been analyzed in terms of the LTE. Results from 5-, 6-, 7- and 8-interval runs have undergone a test estimating the likelihood of interesting O–C variations. 29 detached and 44 contact binaries have passed the final visual tests. Most of the resulting O–C plots have a parabolic shape meaning a linear period increase or decrease. A few objects reveal 3rd degree variations suggesting a long period LTE orbit, of which only a short part is visible in the data set. Finally, three diagrams show evidence of LTE orbits that have periods shorter than the data’s span. These objects have been precisely analyzed using a modified version of the LTE-search algorithm. It uses overlapping intervals and generates more points on the O–C plot than the standard approach, thus revealing the possible shape of the orbit (without increasing the accuracy). Fitted orbits have semi-major axes smaller than 1AU and ≈ 3 year periods.

Obtained O–C plots were compared with known literature data showing compatibility.

The proposed method is well suited for automated data pipelines due to its versatility. It can handle practically any long time-base photometry data and point out most irregularities in eclipse timing.

One thing worth mentioning is that, in general, dealing with O–C requires very precise periods. In our case, the periods came bundled with photometric data from the ASAS Catalogue. If aliases, like $\pm 10, 20, 30\%$ of the correct period, shall occur, the algorithm used to detect O–C variations will give a false signal. It must be therefore used with caution and understanding of the process.

Further simulation work regarding the influence of various light-curve parameters on the detection possibility is in progress.

This work is supported by the Foundation for Polish Science through a FOCUS grant and fellowship, by the European Research Council through the Starting Independent Researcher Grant and Polish MNiSW grant no. N N203 3020 35.

This paper has been typeset from a $\text{\TeX}/\text{\LaTeX}$ file prepared by the author.

REFERENCES

Cordes J. M., Kramer M., Lazio T. J. W., Stappers B. W., Backer D. C., Johnston S., 2004, *New Astronomy Review*, 48, 1413
 Dolez N., Vauclair G., Chevreton M., 1983, *A&A*, 121, L23
 Friedrich S., Zinnecker H., Correia S., Brandner W., Burleigh M., McCaughrean M., 2007, in Napiwotzki R., Burleigh M. R., eds, *15th European Workshop on White Dwarfs Vol. 372 of ASP Conf. Ser., Search for Giant Planets around White Dwarfs with HST, Spitzer, and VLT.* p. 343
 Hulse R. A., Taylor J. H., 1975, *ApJ*, 195, L51
 Konacki M., Wolszczan A., 2003, *ApJ*, 591, L147
 Lee J. W., Kim S., Kim C., Koch R. H., Lee C., Kim H., Park J., 2009, *AJ*, 137, 3181

Mukadam A. S., Mullally F., Nather R. E., Winget D. E., 2004, *ApJ*, 607, 982
 Mullally F., Winget D. E., De Gennaro S., Jeffery E., Thompson S. E., Chandler D., Kepler S. O., 2008, *ApJ*, 676, 573
 Nather R. E., Mukadam A. S., 2004, *ApJ*, 605, 846
 Paczynski B., 1997, in Ferlet R., Maillard J.-P., Raban B., eds, *Variables Stars and the Astrophysical Returns of the Microlensing Surveys The Future of Massive Variability Searches.* p. 357
 Paczynski B., Szczygiel D., Pilecki B., Pojmanski G., 2006, *MNRAS*, 368, 1311
 Pilecki B., Fabrycky D., Poleski R., 2007, *MNRAS*, 378, 757
 Pojmanski G., 2002, *Acta Astronomica*, 52, 397
 Press W. H., Teukolsky S. A., Vetterling W. T., Flannery B. P., 1992, *Numerical recipes in C. The art of scientific computing.* Cambridge: University Press, 1992, 2nd ed.
 Qian S., 2003, *MNRAS*, 342, 1260
 Ribas I., 2005, in C. Sterken ed., *The Light-Time Effect in Astrophysics: Causes and cures of the O-C diagram Vol. 335 of ASP Conf. Ser., Combining Astrometry and Light-time Effect: Low-mass Companions around Eclipsing Systems.* p. 55
 Richer H. B., Ibata R., Fahlman G. G., Huber M., 2003, *ApJ*, 597, L45
 Sigurdsson S., Richer H. B., Hansen B. M., Stairs I. H., Thorsett S. E., 2003, *Sci*, 301, 193
 Sterken C., 2005a, in C. Sterken ed., *The Light-Time Effect in Astrophysics: Causes and cures of the O-C diagram Vol. 335 of ASP Conf. Ser., Binary Pulsars, General Relativity and Light-Time Effects.* p. 215
 Sterken C., 2005b, in C. Sterken ed., *The Light-Time Effect in Astrophysics: Causes and cures of the O-C diagram Vol. 335 of ASP Conf. Ser., Ole Roemer and the Light-Time Effect.* p. 181
 Wolszczan A., Frail D. A., 1992, *Nat*, 355, 145
 Zasche P., 2005, *Ap&SS*, 296, 127